RGNZ/MGPB

Specific energy consumption of material handling by excavator in the quarrying of crushed stone

Rudarsko-geološko-naftni zbornik
(The Mining-Geology-Petroleum Engineering Bulletin)
UDC: 622:621
DOI: 10.17794/rgn.2023.1.8

Original scientific paper

Vjekoslav Herceg[1]; Mario Klanfar[2]; Karolina Herceg[3]; Dubravko Domitrović[4]

[1] *University of Zagreb, Faculty of mining, geology and petroleum engineering, Pierottieva 6, Zagreb, https://orcid.org/0000-0002-5706-9135*
[2] *University of Zagreb, Faculty of mining, geology and petroleum engineering, Pierottieva 6, Zagreb, https://orcid.org/0000-0003-1629-873X*
[3] *University of Zagreb, Faculty of mining, geology and petroleum engineering, Pierottieva 6, Zagreb, https://orcid.org/0000-0002-3450-4296*
[4] *University of Zagreb, Faculty of mining, geology and petroleum engineering, Pierottieva 6, Zagreb, https://orcid.org/0000-0001-9861-8471*

Abstract

A hydraulic excavator is widely used in crushed stone quarries to perform many different operations. Previous research on material handling by excavators is most often based on laboratory testing and observation of soil materials and the digging forces in them. These results are very difficult to transfer to fieldwork during the quarrying process. Therefore, in this work, the energy consumption of an excavator while working in typical materials for a crushed stone quarry was investigated. The field measurements were performed on overburden, blasted rock material, boulders, and two different crushed materials. Energy consumption was observed only during the portion of the cycle in which the bucket digs the material. In this way, the energy consumption was mainly related to the properties of the material. The highest energy consumption was found for blasted rock material, lower in overburden, and the lowest for boulders and crushed materials. These results are important for organizing an optimal distribution of machines according to the work tasks in the quarry and ultimately for energy savings.

Keywords:
mining; excavator; quarry; energy consumption

1. Introduction

Crushed stone quarries are one of the most common types of open pit mines in the world (**NIOSH, 2022**). These quarries are generally developed in a benching system and are mainly mined by drilling and blasting. The hydraulic excavator is an indispensable machine for performing various technological operations at such sites (**Kujundžić et al., 2021**). The multifunctionality of the excavator in the form of the ability to connect various tools significantly expands the range of applications. The most common excavator tool is the bucket, which is used for digging, moving, loading, and feeding various materials. Excavators are used in a variety of jobs, which includes rock material with different properties, especially in smaller quarries where it is not profitable to have a separate excavator for each job. At its simplest, there are two types of materials in a quarry: useful mineral or raw material and overburden. Each of these materials can be in different forms. The raw material is blasted rock of varying grain composition, depending on the quality of the blasting, which undergo crushing and sieving. The overburden may be of different soil compositions and water content or mixed with rock material in a certain ratio. Therefore, we find several materials in the quarry for which different operating parameters of the excavator can be expected due to different physical and mechanical properties. The material properties are important for the interaction of soil and tool, which is related to the energy consumption during digging. Numerous studies have investigated soil-tool interaction with respect to excavator automation. Some of the studies include experiments in the laboratory (**Althoefer et al., 2009, King et al., 2011**) or in the field (**Zhao et al., 2020**), and some of them were for the purpose of developing a better model for identifying soil parameters and predicting forces for automated excavation (**Palomba et al., 2019, Yoseufi Moghaddam et al., 2012**). **Singh (1997)** defines two main problems in determining the interaction between a tool (bucket or blade) and the soil. The first issue is what forces act, how the soil moves and settles, and how much soil ends up in the bucket. The second issue is what resistive forces the bucket is subjected to during the excavation. **Luengo et al., (1998)** presented an on-line method for estimating soil parameters based on measured force data. **Lipsett and Moghaddam (2011)** emphasize that it is possible to estimate soil parameters by modeling the rigid-body dynamics of the machine carrying the tool and measuring

Corresponding author: Vjekoslav Herceg
e-mail address: vjekoslav.herceg@rgn.hr

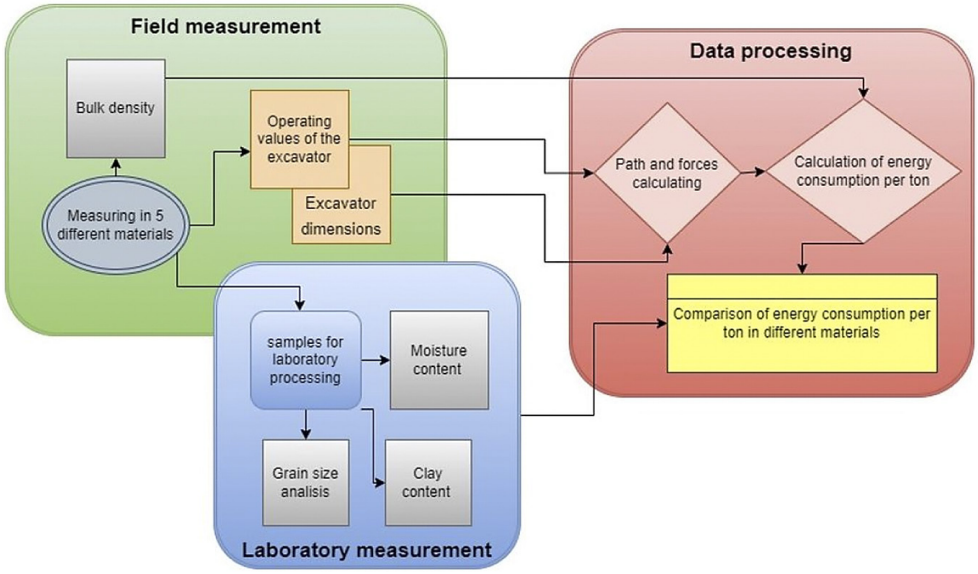

Figure 1: Graphic presentation of research methodology

its motions and interaction forces. Care should be taken to collect data during the digging process. Many studies have attempted to define a soil model that can be used to estimate soil parameters based on measurements of the forces acting on an excavator bucket (**Tan et al., 2005, Bennett et al., 2016**). **Dadhich et al. (2016)** pointed out that a reliable model of bucket-soil interaction model has not yet been achieved. One of the reasons for this is the lack of experimental tests with real field materials and detailed measurements of force and movement of an excavator tool. **Zhao et al. (2020)** conducted soil box and field experiments to validate the proposed fundamental earthmoving equation for identifying soil parameters and predicting force. They performed laboratory tests in five soil types: sand, clayey sand, loam, silty loam, and heavy clay. The field tests and experimental results agree well with the predicted results. The authors stress the importance of extending the tests to other materials.

The laboratory tests are very useful for the theoretical study of soil-tool interaction, but do not give a complete picture of digging under real conditions. There are two additional factors that affect the digging forces of an excavator under real conditions. When digging under real conditions, the material is not homogeneous and the digging path is different for every cycle. Therefore, it is necessary to measure the forces in real operation of an excavator during multiple cycles to capture more influencing factors. It is also necessary to measure the digging path to determine the energy consumption. Energy consumption or work represents an effective force and determines productivity more accurately than the force itself (**Komissarov et al. 2016**).

This paper presents the study of the difference between energy consumption in digging in five types of materials found in quarries at different mining stages. **Jassim et al. (2018)** studied the energy consumption of excavators. They used neural network models to determine the optimal excavators for earthwork projects to reduce energy consumption and CO_2 emissions. **Brînas et al. (2018)** present the model for reducing specific energy consumption on a bucket wheel excavator in coal and overburden excavation. They only considering the specific energy required to cut the material. **Juza and Hermanek (2022)** introduce innovative modifications to the hydraulic system of the telescopic excavator, which achieved significant energy savings during operation.

According to previous studies, we can conclude that energy savings during excavator operation can be achieved by modifying the machine itself, optimizing the operation of the machine, and optimal organization of work.

The idea of this study is that after comparing the energy consumption for different materials in the quarry, we can obtain a basis for the optimal distribution of the work tasks of the excavator in the quarry.

The research approach by stages is graphically shown in **Figure 1.**

2. Research methodology

2.1. Field measurement

The field measurements were carried out in a crushed stone quarry named "Špica", located in the northern part of Croatia, sixty kilometres northeast of Zagreb, near the town of Novi Marof. The predominant rock in the deposits is limestone and dolomitic limestone, dolomite is less present. With the progress made so far, the quarry has been developed in 5 benches with a height of 25 to 30 m and a berm width of 10 to 30 m. The working bench is located at an altitude of 213 to 216 m a.s.l.

Table 1: Technical data of the excavator

Hydraulic excavator DOOSAN DX300LCA	
Manufacturing year	2018
Engine Power	146 kW(193 HP) @ 1,900 rpm
Engine Fuel	Diesel
Operational Weight	29,600 kg
Bucket Capacity	1.12 m^3
Boom/ arm/ bucket length	6.25/ 2.52/ 1.65 m
Max. digging reach/ depth/ height	10.75/ 7.36/ 10.33 m
Hydraulic pump capacity	2 x 247 l/min

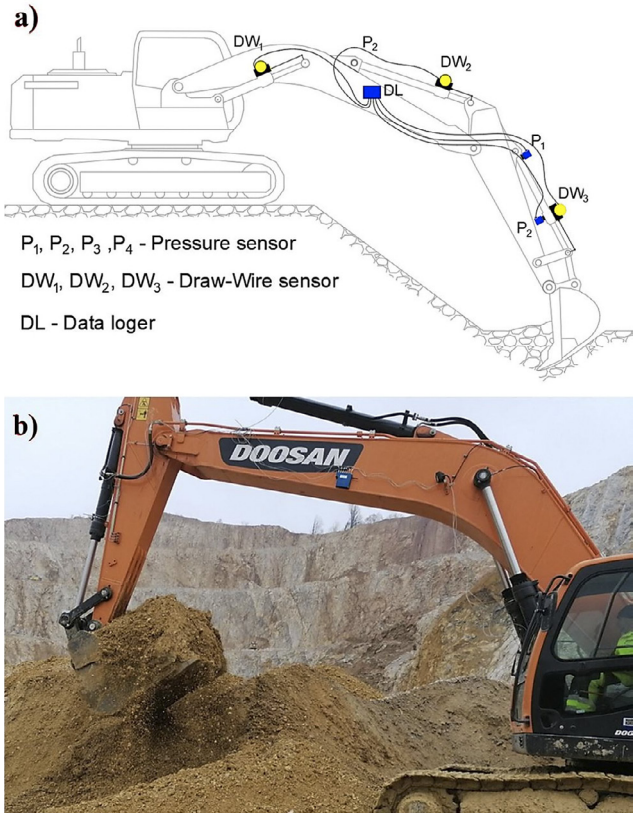

Figure 2: a) The setup of the measurement system (**Klanfar et al., 2019**), b) Excavator on the field

Drilling and blasting are used to extract the rock mass. The blasted material is lowered by gravity onto the working bench and from there transported to the crusher. In the crusher, the material is then crushed down into the required commercial fractions. The products from this quarry are widely used in civil engineering and construction.

2.2. Excavator properties

The operation of a hydraulic excavator consists of work cycles consisting of successive repetitions of digging, lifting, swinging, and dumping the bucket load. Many authors studied the work cycles of excavators, trying to determine as precisely as possible the boundaries between the different parts of a cycle (**Lee et al. 2008, Du et al. 2016**).

To get detailed insight into the work of the excavator, it is necessary to know the trajectory of the tool movement and the forces that occur. This requires measurements of the pressure and displacement of the hydraulic actuators. The measurements were performed on an excavator shown in **Figure 2 – b**, whose technical data are listed in **Table 1**. The setup of the measurement system is shown in **Figure 2 - a**.

The measurement system was setup with two hydraulic pressure transmitters (**Wika A-10**), which were attached to the bucket cylinder, to the boom pressure line and to the upper pressure line of the cylinder. Draw wire displacement sensors (**Microepsilon WPS-2300-MK88**) were mounted on each cylinder. A portable datalogger (battery powered) was used to collect data from all sensors at a sampling rate of 10 Hz. The system was previously tested, and its accuracy and main characteristics were determined as shown in **Table 2** (**Klanfar et al., 2019**). The accuracy of the sensor is expressed as a percentage of Full-Scale Output (%FSO)

Table 2: Measurement system characteristics

	Cylinder pressure	Cylinder displacement
Accuracy	0.026 % FSO	0.087 % FSO
Resolution	0.15 bar	0.58 mm
Range	0–500 bar	0–2400 mm

All cylinder's displacements were used to calculate the bucket trajectory, kinematics, and required spatial coordinates (Chapter 3, Data processing). In conjunction with the kinematics, the pressure of the bucket cylinders was used to calculate the forces on the teeth of the bucket, which serve as the interaction point between the bucket and the rock material during the cycle. The pressure in the boom cylinders was used to determine the mass of the bucket load in each cycle. Further processing of this data yielded the digging energy and bucket fill factor.

Measurements were made in five rock types, with measurement and operating conditions kept constant as much as possible. All measurements were made with a single excavator, operated by the same person, performing a typical cycle of digging, lifting, swinging and dumping. For each material type, data were collected from an average of 20 cycles with a total duration of 250 to 320 s.

2.3. Materials

Five different types of material were used to measure parameters of excavator digging. The types of materials and their properties are listed in **Table 3**.

The materials were selected at the quarry. The first material was overburden consisting of clay and 20% rock fragments. This material was transported by gravity

Table 3: The types of materials and their properties used to measure excavator parameters

Material	Description	Bulk density (t/m³)	Moisture content (%)	D25 (mm)	D50 (mm)	D75 (mm)	Bucket fill factor
Overburden material	Clay with 20% of rock material	1.78	16.20	-	-	-	1.15
Blasted rock	Limestone (0-400 mm)	1.75	<1	69	162	244	0.99
Boulders	Limestone (100-1000 mm)	-	<1	372	531	800	-
Crushed stone	Limestone (0-40 mm)	1.75	1.73	5	16	30	1.01
Crushed stone with clay	Limestone (0-40 mm) with clay 15%	1.84	2.60	4.8	14	28	1.34

from the upper part of the quarry to the working bench. There it was loaded into trucks by the excavator and taken to a landfill. Measurements were taken while the material was being loaded onto the truck. The second material was blasted rock material that was on the working bench. Boulders too large to enter the primary crusher were pushed aside to be crushed later with a hydraulic hammer. While these boulders were being transported, a second measurement was made. The blasted material that remained after the boulders were removed was loaded into the truck, and during this process the third measurement was taken. Two heaps of crushed rock products were stored on the working bench. One was obtained by crushing blasted rock in a mobile crusher, and the second was obtained by crushing blasted rock contaminated with 15% clay. The fourth and fifth measurements were made on these materials during transport from pile to pile to simulate truck loading.

Figure 3: The bulk density measurement setup

2.3.1. Bulk density

The bulk density (B_d) of the material was determined in the quarry. After measuring the digging forces by an excavator working under real conditions in each material, the bulk density was measured on the same samples using a wooden box of known volume ($Vb = 1\ m^3$) and a dynamometer to measure the mass. The material was loaded into the wooden box and lifted with an excavator. The value of the mass was recorded on the dynamometer, which was connected to the box and the excavator bucket with cargo straps, as shown in **Figure 3**. Before measuring the mass of the full box (m_{fb}), the mass of the empty box (m_{eb}) was measured in the same way. The bulk density (B_d) was calculated according to equation [1].

The bucket fill factor (B_{ff}) was calculated according to equation [2], where (M_m) is the mass of the material in the bucket and (V_b) is the volume of the bucket or the bucket capacity.

$$Bd = \frac{m_{fb} - m_{eb}}{V_b}\left(\frac{t}{m^3}\right) \quad [1]$$

$$Bf_f = \frac{\frac{M_m}{B_d}}{V_b} \quad [2]$$

2.3.2 Laboratory measurements

Samples of overburden and crushed stone products were collected from the quarry and prepared for laboratory testing. Water content and grain size distribution of the samples were determined according to **ASTM D2216-10 (2010)** and **ASTM D 422-63(2007)e1 (2014)**, respectively.

Grain size distribution of blasted rock masses and boulders was determined using "WipFrag" software based on photographs taken during field measurements. The water content of well blasted and rough blasted rock was estimated based on the water absorption of limestone and dolomitized limestone, which is less than 0.25% and not significant for material with such fragment dimensions.

2.4. Data processing

The data output from the measurement system were pressures and displacement positions of cylinders, recorded at 0.1 s intervals. The final values to be presented in this paper are the energy consumption per cycle (*Ep*), and the mass of material in the bucket (M). These values are calculated using the equations explained below.

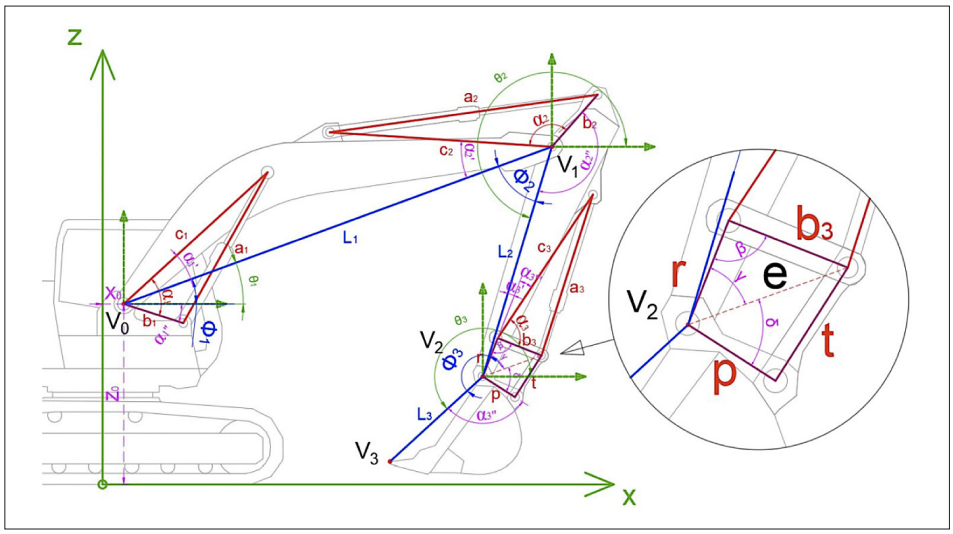

Figure 4: Kinematics of the excavator

The first step in the data processing was to calculate the motion trajectory of the excavator bucket. For this it is necessary to know the kinematics of the excavator. **Koivo A. J. (1994)** presented a detailed calculation of the kinematics of the excavator using a Cartesian rectangular coordinate system with local Denavit–Hartenberg coordinate systems in joints. This solution is also used in this work and is shown in **Figure 4**. The dynamics of the excavator can be explained by the Newton-Euler formulation algorithm using vector equations (**Väihä and Skibniewski, 1993, Assenov et al., 2003**) and trigonometric equations (**Kwon, 2008**) which are also used in this work.

The following equations [3-14] show step by step how the coordinates of the links (boom, arm and bucket) are calculated with the input data of cylinder displacement. All lengths and angles used for the calculation are shown in **Figure 4**. In triangles (a_i, b_i, c_i), where (ai) is the length of the cylinder between the joints and (b_i, c_i) are the fixed lengths between the joints in the construction of the excavator, the objective is to obtain the value of the angle (α_i) according to equation [3]. In a quadrangle (b_3, *r, t, p*) where each side is a fixed length on the excavator, equations [7-10] are used to calculate the angles (, ,) and the length (*e*). () are relative angles between the links of the excavator and () are absolute angles between the links and the horizontal axis with origin in the local coordinate system. The angles are calculated using equations [4,5,6,11,12]. are fixed angles between the axes connecting the joints of the excavator structure shown in **Figure 4**. The coordinates of the top of the links (,) are calculated using equations [13,14] where) is the length of the link.

$$\cos(\alpha_i) = \frac{b_i^2 + c_i^2 - a_i^2}{2 \cdot b_i \cdot c_i} \quad [3]$$

$$\theta_1 = \Phi_1 = \alpha_1 - (\alpha_1' + \alpha_1'') \quad [4]$$

$$\Phi_2 = 360 - (\alpha_2 + \alpha_2' + \alpha_2'') \quad [5]$$

$$\theta_2 = \theta_1 + \varnothing_2 + 180 \quad [6]$$

$$\beta = 180 - (\alpha_3 + \alpha_3''') \quad [7]$$

$$e = \sqrt{r^2 + b_3^2 - 2 \cdot r \cdot b \cdot \cos(\beta)} \quad [8]$$

$$\cos(\gamma) = \frac{e^2 + r^2 - b_3^2}{2 \cdot e \cdot r} \quad [9]$$

$$\cos(\delta) = \frac{e^2 + p^2 - t^2}{2 \cdot e \cdot p} \quad [10]$$

$$\Phi_3 = 360 - (\gamma + \delta + \alpha_3' + \alpha_3'') \quad [11]$$

$$\theta_3 = \theta_2 - 180 + \varnothing_3 \quad [12]$$

$$XV_i = XV_{i-1} + (\cos(\theta_i) * L_i \quad [13]$$

$$ZV_i = ZV_{i-1} + (\cos(\theta_i) * L_i) \quad [14]$$

The force of the bucket cylinder (F_c) was calculated using equation [15], where (P_1, P_2) are the pressures in the cylinder, (*Dc*) is the bore diameter, and (*Dp*) is the rod diameter (see **Figure 5**). The force on the tooth of the bucket (F_R), which is tangential to the digging path, was calculated using equation [16], where (are angles used to calculate the vertical projection of the force on the bucket. The digging path is represented with points (t_i) defined with coordinates (XV_i, ZV_i) of the tooth of the bucket in each measurement point. The distance between two adjacent points (s_i) was calculated using equation [17]. Energy consumption for digging material (*EC*) was calculated using equation [18]. The mass of material (M_m) in the bucket is represented by equation [19]. It was calculated after digging at the beginning of swinging when the axis of the bucket (L_3) was in a horizontal position.

$$F_c = \left(\frac{D_C}{2}\right)^2 * \pi * P_1 - \left(\left(\frac{D_C}{2}\right)^2 * \pi - \left(\frac{D_p}{2}\right)^2 * \pi\right) * P_2 \quad [15]$$

$$F_R = \cos(\lambda) * \frac{F_C * \cos(90-\varphi) * \cos(90-\varepsilon) * p}{L_3} \quad [16]$$

$$s_i = \sqrt{(XV_i - XV_{i-1})^2 + (ZV_i - ZV_{i-1})^2} \quad [17]$$

$$EC = \sum_{i=0}^{n} F_{R_i} * s_i \quad [18]$$

$$M_m = \frac{F_C * \cos(90-\varphi) * \cos(90-\varepsilon) * p}{g} \quad [19]$$

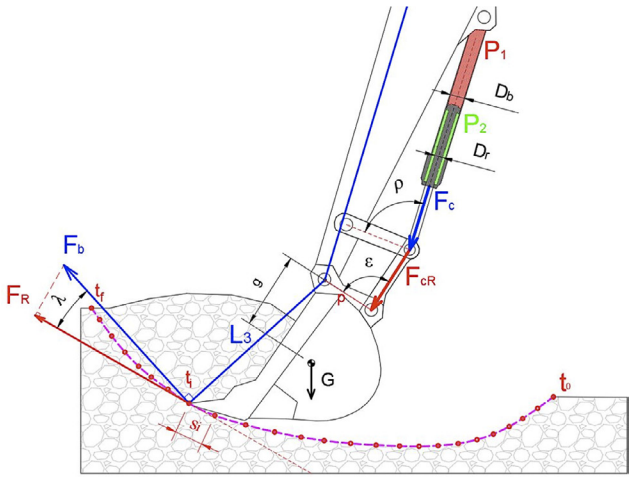

Figure 5: Forces calculation scheme

3. Results and discussion

Digging forces have been studied by many authors (e.g. **Kim et al., 2013, Kusmierczyk and Szlagowski, 2008**). Their goal was usually to optimize the operation of the excavator. They also concluded that the digging forces depend on the type of material. This can also be confirmed in this work. **Figure 6** shows the digging forces for a typical cycle, separately for each material in which the measurements were performed. From the results, it can be concluded that the forces do not behave the same when digging in different types of materials. Considering this, the energy consumption is also different.

Figure 7 shows the digging forces and energy consumption between the measurement points in a typical cycle. The middle part of the curve shows relatively good overlap, but poor overlap of the curves can be seen at the beginning and end of the trench. These differences are due to the fact that the top of the bucket moves faster at these points due to the inclusion of the boom cylinder and covers a greater distance in less time, while the force does not change as much. Therefore, it can be said that energy consumption more accurately describes the process of excavation than just forces. Data measured and compared in this way was not found in literature.

The energy consumption for each material measured is shown in **Figure 8**. The measurement procedure was carried out as described in Section 2.1. For each cycle, only the digging process (bucket filling) was selected without lifting, dumping, and swinging. The average digging energy consumption of all cycles for each material was calculated. The graph shows the average energy consumption per ton of loaded mass in each material. The highest energy consumption was for blasted rock. It can be concluded that this is due to the well size distribution and wide range of grain sizes (0-400 mm) (see **Table 1).**

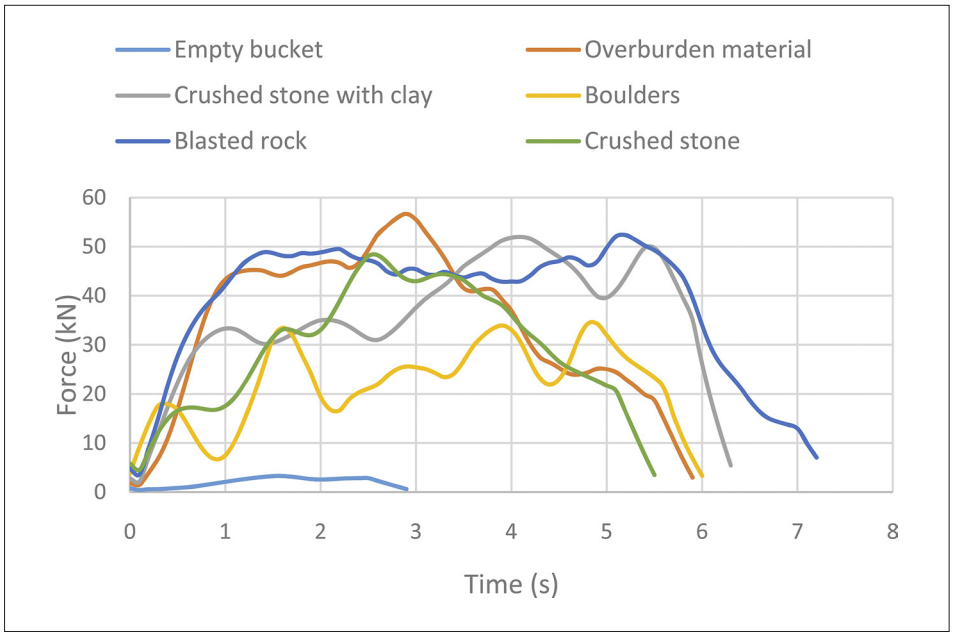

Figure 6: Digging forces

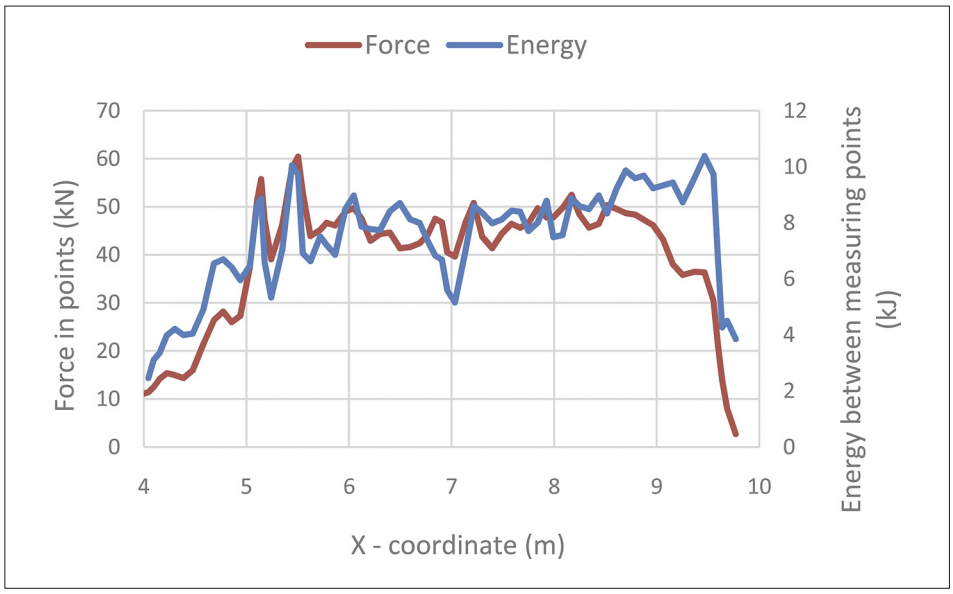

Figure 7: Force and energy by typical digging

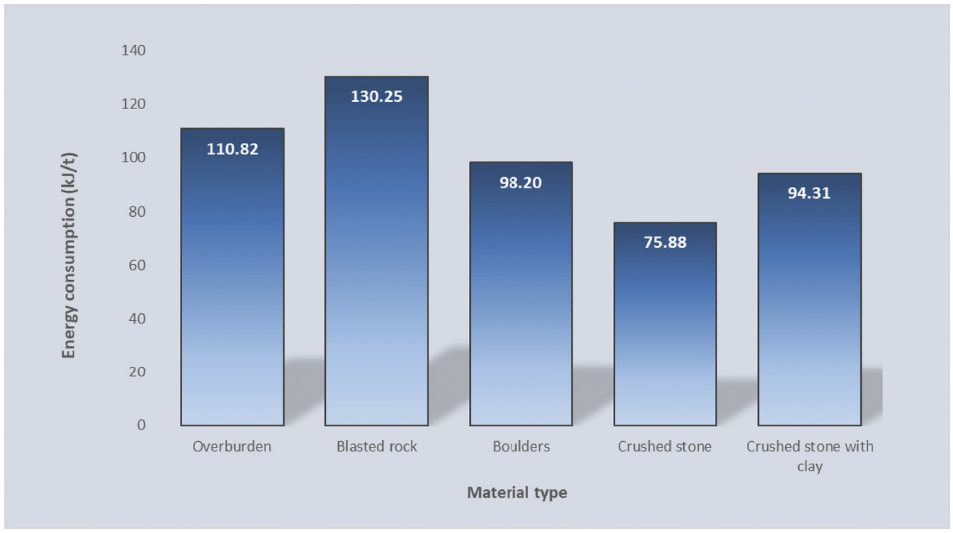

Figure 8: Energy consumption (kJ/t)

The second highest energy consumption was in overburden, which consists of high plasticity clay, so that adhesion forces occur during contact between the soil and the tool, which **Swick and Perumpral (1988)** also mentioned. When measurements were made in boulders, the energy consumption was lower. The reason may be the large size of the fragments and the uniform size distribution, which may cause low friction between the rock fragments and the tool. The lowest energy consumption was found for crushed stone. It can be assumed that the reason is the fine material and the very small size range (0-40 mm), which is also mentioned by **Zhao et al. (2020)**. The difference between crushed stone and crushed stone with clay is about 20%, so 15% clay admixture can play a significant role in energy consumption for this size distribution. These data on energy consumption in digging are very difficult to compare with the results of other authors. There are very few studies in the literature that present these data. **Hippalgaonkar and Ivantysynova (2016)** show the results of the energy of digging per cycle, which are between 20 and 60 kJ, but they use a mini-excavator with unknown bucket volume. With an assumption that a bucket was used that can hold about 0.3 tons of material, then the data can be compared to the results in this paper. **Jassim et al. (2018)** shows the results of energy consumption measurements throughout entire digging cycle when excavating material from depth. They determined energy consumption ranging from 0.6 to 6.3 MJ/m^3. In contrast to them, this article considers only the digging process, which depends mainly on the type of material. The energy for lifting, swinging, and dumping depends on the mass of the material in the bucket and the trajectory of movement. To compare energy consumption for different materials, it is much more accurate to observe the digging itself.

4. Conclusion

The materials considered in this work are closely related to the technological operations in the quarry. It can be concluded that the highest energy consumption in the

use of excavators in the quarry occurs when working with blasted rock material. This can be loading, moving, gravity transport or feeding a mobile crusher. Somewhat less energy is consumed when working in the overburden. Again, this can be loading, moving, or gravity transport. When the excavator separates boulders from the blasted material for crushing with a hydraulic hammer, energy consumption is even lower. The lowest energy consumption occurs when the excavator is operating in crushed material.

Blasted rock material has a wide grain size range and often a well size distribution. These characteristics combined together may be the reason for the high resistance during digging. Materials with a smaller grain size range, such as crushed stone, and uniform size distribution, such as boulders, provide 20 to 40% less digging resistance than the blasted rock material. Overburden, in this case, has a lower energy consumption than blasted rock, but it must be taken into account that it contains mostly clay, which changes its properties significantly with water content variations. The differences in energy consumption between crushed stone with and without clay also suggest that clay in crushed stone may increase excavation resistance. In further research, field measurements should be made on other materials in different quarries to verify these results. It would also be useful to perform measurements at different water contents, which would provide more information about the behaviour of these materials under different atmospheric conditions, which is especially important for overburden.

The first novelty in this article is the approach of the measurement made in real conditions, which is very rare, while the measurement in different materials in the quarry was not found in literature. The novelty of this work is also the verification and comparison of the actual energy consumption of the material manipulation in the quarry. With the help of these findings, it is possible to address the reduction of energy consumption by optimally organizing the work in the quarry. A similar approach was taken by **Jassim et al. (2018)**, whose work investigated the energy consumption at different depths of soil excavation and suggested the optimal choice of machine. **Brînas et al. (2018)** base the reduction of energy consumption on the optimization of the digging operation, while **Juza and Hermanek (2022)** base the reduction of energy consumption on modifications to the hydraulic system of the machines itself. The approach taken in this work can simply help mining engineers and quarry managers save energy by distributing the work tasks in the quarry and evaluating the relative energy/fuel consumption of the different materials.

5. References

Althoefer, K.; Tan, C. P.; Zweiri, Y. H.; Seneviratne, L. D. (2009) Hybrid Soil Parameter Measurement and Estimation Scheme for Excavation Automation, IEEE Transactions on Instrumentation and Measurement, 58(10), 3633-3641. https://doi.org/10.1109/TIM.2009.2018699.

Asenov, E., Bosilkov, E., Dimitrov, R. and Damianv, T., (2003): Kinematics and dinamics of hydraulic excavator. Electrification and Automation in Mines. 46, 47-49.

ASTM D 422-63(2007)e1 (2014): Standard Test Method for Particle-Size Analysis of Soils. West Conshohocken, PA:ASTM International.

ASTM D2216-10 (2010): Standard Test Methods for Laboratory Determination of Water (Moisture) Content of Soil and Rock by Mass. West Conshohocken, PA: ASTM International.

Bennett, N., Walawalkar, A., Heck, M., Schindler, C. (2015): Integration of digging forces in a multy-body.system model of an excavator. Proceedings of the Institution of Mechanical Engineers Part K Journal of Multi-body Dynamics, Volume 230(2), 159-177. https:// 10.1177/14644193 15592081.

Brînas, I., Andras, A., Radu, S.M., Popescu, F.D., Andras, I., Marc, B.I., Cioclu, A.R. (2021): Determination of the Bucket Wheel Drive Power by Computer Modeling Based on Specific Energy Consumption and Cutting Geometry. Energies 14, 3892. https://doi.org/10.3390/en14133892

Centers for disease control and prevention (2022): NIOSH Mining. URL: https://wwwn.cdc.gov/niosh-mining/MMWC /Mine

Dadhich, S.; Bodin, U.; Andersson, U. (2016): Key challenges in automation of earth-moving machines. Automation in Construction. 68. https://doi.org/10.1016/j.autcon.2016.05.009.

Du, Y.; Dorneich, M. C.; Steward, S. (2016): Virtual operator modeling method for excavator trenching, Automation in Construction, 70, 14-25. https://doi.org/10.1016/j.autcon.2016.06.013.

Hippalgaonkar, R., Ivantysynova, M., (2016): Optimal Power Management of Hydraulic Hybrid Mobile Machines – Part I: Theoretical Studies, Modeling and Simulation. Journal of Dynamic Systems Measurement and Control. 138. https://doi.org/10.1115/1.4032742.

Jassim, H.S.H.; Lu, W.; Olofsson, T. (2018): Quantification of Energy Consumption and Carbon Dioxide Emissions During Excavator Operations. In: Smith, I., Domer, B. (eds) Advanced Computing Strategies for Engineering. EG-ICE 2018. Lecture Notes in Computer Science, 10863. 431–453. https://doi.org/10.1007/978-3-319-91635-4_22

Juza, M.; Hermanek, P. (2022): Study of the energy efficiency of the USD 214 Excavator hydraulic system. MM Science journal. October, 2022. DOI : 10.17973/MMSJ.2022_10_2022077

Kim, B. Y., Ha, J., Kang, H., Kim, P. Y., Park, J., Park, F.C., (2013): Dynamically optimal trajectories for earthmoving excavators. Automation in Construction. 35, 568–578. https://doi.org/10.1016/j.autcon.2013.01.007

King, R.H.; Van Susante, P.; Gefreh, M.A. (2011): Analytical models and laboratory measurements of the soil–tool interaction force to push a narrow tool through JSC-1A lunar simulant and Ottawa sand at different cutting depths, 85-95. https://doi.org/10.1016/j.jterra.2010.07.003.

Klanfar, M., Herceg, V., Kuhinek, D., & Sekulić, K. (2019). Construction and testing of the measurement system for excavator productivity. Rudarsko-geološko-Naftni Zbornik, 34(2). https://doi.org/10.17794/rgn.2019.2.6

Koivo, A. J. (1994): Kinematics of excavators (backhoes) for transferring surface material. Journal of Aerospace Engineering. 7, 17–32. https://doi.org/10.1061/(asce)0893-1321(1994)7:1(17).

Komissarov, A.P.; Lagunova, Y.A.; Lukashuk, O.A. (2016): Evaluation of Single-bucket Excavators Energy Consumption, Procedia Engineering, 150, 1221-1226. https://doi.org/10.1016/j.proeng.2016.07.239.

Kujundžić, T.; Klanfar, M.; Korman, T.; Briševac, Z. (2021): Influence of Crushed Rock Properties on the Productivity of a Hydraulic Excavator. Appl. Sci. 2021, 11, 2345. https://doi.org/10.3390/app11052345.

Kwon, S. K., Kim, J. J., Jung, Y. M., Jung, C. S., Lee, C. D. and Yang, S. Y., (2008): A hydraulic simulator for an excavator. JFPS International Symposium on Fluid Power, 7-3, 611-616. https://doi.org/10.5739/ISFP.2008.611

Lee, S. L., Chang, P. H., (2012): Modeling of a hydraulic excavator based on bond graph method and its parameter estimation. Journal of Mechanical Science and Technology. 26, 195-204. https://doi.org/10.1007/s12206-011-0938-2

Lee, S.; Hong, D.; Park, H.; Bae, J. (2008): Optimal path generation for excavator with neural networks based soil models, IEEE International Conference on Multisensor Fusion and Integration for Intelligent Systems, 632-637. https://doi.org/10.1109/MFI.2008.4648015.

Lipsett, M.G.; Moghaddam, R.Y. (2011). Modeling Excavator-Soil Interaction. In: Wan, R., Alsaleh, M., Labuz, J. (eds) Bifurcations, Instabilities and Degradations in Geomaterials. Springer Series in Geomechanics and Geoengineering, 0, 347–366 https://doi.org/10.1007/978-3-642-18284-6_19

Luengo, O.; Singh, S.; Cannon, H. (1998): Modeling and identification of soil-tool interaction in automated excavation. IEEE International Conference on Intelligent Robots and Systems, 3, 1900 - 1906. https://doi.org/10.1109/IROS.1998.724873.

Palomba, I.; Richiedei, D.; Trevisani, A.; Sanjurjo, E.; Luaces, A.; Cuadrado, J. (2019): Estimation of the digging and payload forces in excavators by means of state observers. Mechanical Systems and Signal Processing, 134. https://doi.org/10.1016/j.ymssp.2019.106356.

Singh, S. (1997): The State of the Art in Automation of Earthmoving. Journal of Aerospace Engineering, 10(4), https://doi.org/10.1061/(ASCE)0893-1321(1997)10:4(179).

Swick, W.C., Perumpral, J.V., (1988): A model for predicting soil-tool interaction, Journal of Terramechanics, Volume 25(1), 43-56. https://doi.org/10.1016/0022-4898(88)90061-4.

Tan, C.; Zweiri, Y.; Althoefer, K.; Seneviratne, L. (2005): Online Soil Parameter Estimation Scheme Based on Newton–Raphson Method for Autonomous Excavation. Mechatronics, IEEE/ASME Transactions on, 10, 221 - 229. https://doi.org/10.1109/TMECH.2005.844706.

Vaiha, P. K. and Skibniewski, M. J., (1993): Dynamic model of excavator. Aerospace Engineering, 6, 148-158. https://doi.org/10.14279/depositonce-6413

Yoseufi Moghaddam, R., Kotchon, A., Lipsett, M.G. (2012): Method and apparatus for on-ine estimation of soil parameters during excavation. Journal of Terramechanics, 49, 173-181. https://doi.org/10.1016/j.jterra.2012.05.002

Zhao, Y.; Wang, J.; Zhang, Y.; Luo, C. (2020): A Novel Method of Soil Parameter Identification and Force Prediction for Automatic Excavation, IEEE Access, 8, 11197-11207, https://doi.org/10.1109/ACCESS.2020.2965214.

SAŽETAK

Specifična potrošnja energije kopanja materijala bagerom pri dobivanju tehničko-građevnoga kamena

Hidraulični bager ima široku primjenu u obavljanju različitih poslova na kamenolomima tehničko-građevnoga kamena. Dosadašnja istraživanja rada bagera u različitim materijalima najčešće su bazirana na laboratorijskim ispitivanjima provedenim na uzorcima tla te na promatranju sila kopanja u njima. Takve rezultate vrlo je teško primijeniti na realan rad bagera u kamenolomu. U sklopu ovoga istraživanja provedeno je ispitivanje potrošnje energije prilikom rada bagera na tipičnim materijalima u kamenolomu. Terenska mjerenja izvedena su na otkrivci, odminiranoj stijenskoj masi, blokovima i dvjema različitim frakcijama drobljenoga materijala. Potrošnja energije promatrana je samo tijekom dijela ciklusa u kojemu lopata kopa materijal. Na taj način potrošnja energije najviše ovisi o svojstvima materijala. Najveća potrošnja energije izmjerena je pri radu u odminiranoj stijenskoj masi, nešto niža u otkrivci, zatim u blokovima te najniža u drobljenome materijalu. Ovi rezultati važni su za organizaciju optimalne raspodjele strojeva po radnim zadatcima u kamenolomu te u konačnici za uštedu energije.

Ključne riječi:
rudarstvo, bager, kamenolom, potrošnja energije

Author's contribution

Vjekoslav Herceg (1) (Assistant) participated in initiating the idea and developing a methodological approach, conducted the field work, provided literature review, performed data analysis and the interpretation and presentation of the results. **Mario Klanfar (2)** (Associate Professor) participated in initiating the idea and developing a methodological approach, performed the field work, provided the measurement system description and helped with the presentation of the results. **Karolina Herceg (3)** (Postdoctoral Researcher) performed the laboratory data analysis and literature review regarding soil-tool interaction. **Dubravko Domitrović (4)** (Associate Professor) performed the field work, conducted literature review and helped with the presentation of the results.